



Quantitative MR Perfusion for the Differentiation of Recurrence and Radionecrosis in Hypoperfusion and Hyperperfusion Brain Metastases After Gamma Knife Radiosurgery

Yang Yunqi^{1†}, Niu Aihua^{2†}, Zheng Zhiming², Liu Yingchao², Wang Qiang³, Ming Yang^{4*} and Zhang Yi^{5*}

¹ Department of Neurosurgery, Dongming People's Hospital, Heze, China, ² Department of Neurosurgery, Shandong Provincial Hospital Affiliated to Shandong First Medical University, Jinan, China, ³ Department of Human Resources, Shandong Provincial Hospital Affiliated to Shandong First Medical University, Jinan, China, ⁴ Department of Neurosurgery, The Affiliated Hospital of Southwest Medical University, Luzhou, China, ⁵ Department of Radiology, Shandong Provincial Hospital Affiliated to Shandong First Medical University, Jinan, China

OPEN ACCESS

Edited by:

Ives R. Levesque,
McGill University, Canada

Reviewed by:

Stefan Schob,
University Hospital in Halle, Germany
David Mathieu,
Université de Sherbrooke, Canada

*Correspondence:

Zhang Yi
zhangyisd@139.com
Ming Yang
my520644@163.com

[†]These authors have contributed
equally to this work and share first
authorship

Specialty section:

This article was submitted to
Applied Neuroimaging,
a section of the journal
Frontiers in Neurology

Received: 30 November 2021

Accepted: 21 February 2022

Published: 18 March 2022

Citation:

Yunqi Y, Aihua N, Zhiming Z,
Yingchao L, Qiang W, Yang M and Yi Z
(2022) Quantitative MR Perfusion for
the Differentiation of Recurrence and
Radionecrosis in Hypoperfusion and
Hyperperfusion Brain Metastases
After Gamma Knife Radiosurgery.
Front. Neurol. 13:823731.
doi: 10.3389/fneur.2022.823731

Objectives: Dynamic susceptibility contrast perfusion weighted imaging (DSC-PWI) plays an important role in the differential diagnosis between radionecrosis and recurrence of brain metastases (BMs) after gamma knife radiosurgery (GKRS). While the perfusion condition of preliminary hyperperfusion and hypoperfusion BMs when recur has not been studied, as well the separating performance of quantitative DSC-PWI in both kinds of BMs.

Methods: From February 2017 to October 2019, quantitative DSC-PWI was performed in patients with untreated BMs in this observational study. Patients were assigned to hyperperfusion and hypoperfusion group according the quantitative cerebral blood volume (qCBV). During follow-up after GKRS, patients with a diagnostic pitfall of radionecrosis and recurrence accepted second quantitative DSC-PWI. Final diagnosis was based on the histological results or follow-up results. Receiver operating curve analysis was used to explore the performance of qCBV.

Results: Twenty-nine patients (mean age: 61.3 ± 9.4 years old; male/female: 13/16) were assigned to the group of hypoperfusion group, and 26 patients (mean age: 58 ± 10.4 years old; male/female: 14/12) to hyperperfusion group. The mean qCBV values between hypoperfusion and hyperperfusion groups when recurred were not significantly different (3.17 ± 0.53 ml/100 g vs. 3.27 ± 0.47 ml/100 g, $p = 0.63$). qCBV was feasible to separate radionecrosis and recurrence in both groups (AUC=0.94 and AUC=0.93, separately).

Conclusion: Both premilitary hyperperfusion and hypoperfusion BMs would transform to a high microvascular density when recurs. qCBV is feasible to distinguish radionecrosis and recurrence among both kinds of BMs after GKRS.

Keywords: brain metastases (BMs), MR perfusion, radionecrosis (RN), gamma knife radiosurgery (GKRS), recurrence

INTRODUCTION

Brain metastases (BMs) are among the most common tumors in the central nervous system, with a poor prognosis and high morbidity and mortality (1). Radiation therapy is an alternative for subsequent treatment. In recent years, gamma knife radiosurgery (GKRS) has become an increasingly popular choice for patients diagnosed with BM because it leads to only limited treatment-induced morbidity (2). Even so, radionecrosis can still occur among some patients after GKRS (3), which is difficult to separate from recurrence using conventional structural images.

Dynamic susceptibility contrast perfusion weighted imaging (DSC-PWI) is one of the most commonly used methods in the differential diagnosis of radionecrosis and tumor recurrence for both gliomas and BMs (4–6). The popular interpretation is that tumor recurrence is characterized by increased angiogenesis, but radionecrosis is not (4, 6, 7). However, in clinical practice, doubts persist. High-grade gliomas are accompanied by obvious angiogenesis; therefore, recurrent high-grade gliomas show an obviously increased cerebral blood volume (CBV) in the irradiated area. However, as the two most common types (8), brain metastases originating from lung and breast tumors are considered hypoperfusion tumors, which are different from high-grade gliomas (9, 10). Theoretically, recurrent BMs would not show increased CBV because these BMs are hyperperfused before GKRS treatment.

Previous studies did not separate recurrent BMs into hyperperfusion and hypoperfusion BMs before analysis (5, 9–12). In other words, they did not report the untreated perfusion conditions of recurrent BMs. Therefore, it is still unknown whether hypoperfusion BMs transform to hyperperfusion BMs when they recur. The technical limitations of conventional DSC-PWI may be a response to this uncertain condition because rCBV is a qualitative parameter, which is not qualified enough for comparisons across different scanning times (13). Quantitative DSC-PWI is urgent for this work. Currently, the Bookend DSC-PWI technique, which uses pre- and postcontrast T1 maps to calibrate a conventional DSC sequence, is a quantitative DSC-PWI technique that enables comparisons across different scanning times (14, 15).

With the help of quantitative CBV (qCBV) derived from Bookend DSC-PWI, this study aimed to investigate the perfusion condition of hyperperfusion and hypoperfusion BMs when they recur, as well the separation performance of qCBV in both kinds of BMs.

MATERIALS AND METHODS

Study Population

From February 2017 to October 2019, 340 patients with BMs were treated by GKRS in Shandong Provincial Hospital Affiliated to Shandong First Medical University. Patients who met the inclusion criteria were enrolled in this retrospective study. The inclusion criteria were as follows: [1] histopathological diagnosis of primary cancer; [2] target BM lesions that met the criterion of Response Assessment in Neuro-Oncology Brain Metastases

(RANO-BM); [3] treatment by GKRS; [4] newly enhanced lesions or enlarged enhanced lesions were revealed inside the irradiated nidus after injection of contrast agent during follow-up MRI examination; and [5] postirradiation period > 5 months. Among the 340 patients, 96 met the inclusion criteria.

However, 41 patients were excluded for the following reasons: [1] no qCBV map before GKRS ($n = 16$); [2] no qCBV map when diagnosed with recurrence or radionecrosis ($n = 11$); [3] unqualified MRI data (e.g., severe head motions, $n = 5$); [4] no follow-up MRI data or pathological results ($n = 9$). Finally,

TABLE 1 | The summarized information of all enrolled populations.

	Hyperperfusion group	Hypoperfusion group	P value
Age, years	58 ± 10.4	61.3 ± 9.4	0.23
Gender, male/female	14/12	13/16	0.59
Primary tumor, n			0.006
Lung	8	18	
Breast	4	8	
Kidney	9	0	
Digestive tract	2	2	
Melanoma	3	1	
Locations, n			0.94
Frontal	6	7	
Parietal	8	7	
Temporal	3	5	
Occipital	3	4	
Cerebellum	5	4	
Brainstem	1	2	
KPS, median [IQR]	70 [70,90]	70 [70,90]	0.63
MD, median [IQR]	2.3 [1.7, 2.5]	2.5 [1.7, 3.2]	0.27
Dose, median [IQR]	18 [18, 21]	18 [18, 21]	0.71

KPS, Karnofsky performance status; IQR, interquartile range; MD, maximum diameter.

TABLE 2 | The detailed results of comparisons between two groups.

Primary tumor	Histological subtype	Hyperperfusion group	Hypoperfusion group
Lung	Squamous carcinoma	3	7
	Adenocarcinoma	2	9
	small cell lung cancer	3	2
Breast	Invasive ductal carcinoma	2	4
	Invasive lobular carcinoma	2	2
	Adenocarcinoma	0	2
Kidney	Renal clear cell carcinoma	7	0
	Papillary renal cell carcinoma	2	0
Digestive tract	Adenocarcinoma	2	2
Melanoma	Superficial spreading melanoma	3	1

TABLE 3 | The detailed results of comparisons between two groups.

	Hyperperfusion group	Hypoperfusion group	<i>P</i> value
Recurrence	2.89 ± 0.58	3.0 ± 0.58	0.62
Radionecrosis	1.59 ± 0.31	1.68 ± 0.26	0.45
ΔqCBV _{recurrence}	0.15 [-0.3, 0.2]	2.0 [1.6, 2.3]	<0.001
ΔqCBV _{radionecrosis}	-1.92 ± -0.68	0.18 ± 0.39	<0.001

55 patients (age: 59.8 ± 9.9 years old, male/female: 27/28) were enrolled in this retrospective study.

Written informed consent was obtained from all patients before commencement of the study and after receiving approval from the hospital's ethical committee. All experiments were performed in compliance with the Declaration of Helsinki.

MRI Protocol

All patients underwent MR scans on a MAGNETOM 3T scanner (Skyra, Siemens, Erlangen, Germany) using a 20-channel head-neck coil. The MR exam included a routine protocol for brain examination (T2WI, precontrast T1WI, and T2-FLAIR) and a prototype Bookend DSC-PWI sequence called ScalePWI. ScalePWI could be acquired only after the approval of Siemens Healthineers. The ScalePWI sequence merged the pre- and postcontrast T1 mapping into the GRE-EPI sequence for DSC-PWI. The details of the descriptions of ScalePWI were described previously (16). The imaging parameters of ScalePWI were as follows: TR/TE 1,600 ms/30 ms, bandwidth 1,748 Hz/pixel, 21 axial slices, field of view (FOV) 220 × 220 mm, voxel size 1.8 × 1.8 × 4 mm³, slice thickness 4.0 mm, and a flip angle (FA) of 90 degrees. For each slice, 50 measurements were acquired for DSC-PWI analysis. After 46 s of injector delay, 0.2 mmol per kg bodyweight of contrast agent (Gd-DTPA, Magnevist; Schering, Berlin, Germany) was administered, followed by a 20-ml saline flush. An injection velocity of 4.0 ml/s was introduced in this study. Quantification of cerebral blood volume is based on the Bookend technique, where the value of qCBV is dependent on the change of white matter before and after the injection of

$$\text{contrast agent: } CBV_{WM} = \frac{\left(\frac{1}{T_1^{Post}} - \frac{1}{T_1^{Pre}}\right)_{WM}}{\left(\frac{1}{T_1^{Post}} - \frac{1}{T_1^{Pre}}\right)_{Blood}} \times 100\%, \text{ quantification}$$

of CBV_{WM}: $qCBV_{WM} = WCF(R_1) \times \frac{1}{\rho} \times \frac{1-Hct_{IV}}{1-Hct_{SV}} \times CBV_{WM}$, where $WCF(R_1) = 8.2 \times 10^{-3} R_1^2 + 0.25 R_1 + 0.51$, $\rho Hct_{IV} / Hct_{SV} R_1$ were all constant values. The qCBV of each voxel was calculated by the following functions: $qCBV = rCBV \times \frac{qCBV_{WM}}{rCBV_{WM}}$. Unit of qCBV is ml/100 g.

Then, a postcontrast T1-weighted sequence with the same slices as ScalePWI was performed. The imaging parameters were as follows: TR/TE 250/2.5 ms, TI 900 ms, FOV 220 × 220 mm, slice thickness 4 mm, and FA 70 degrees. The imaging protocol was the same for all patients.

Tumor Segmentation

Target lesions were chosen based on the principle of RANO-BM (17), but only the largest lesion was chosen for one patient. For both untreated BM lesions and follow-up BM lesions, regions of

interest (ROIs) were drawn completely by hand to only cover the enhancing area inside the lesions on postcontrast T1W images, avoiding major cortical vessels adjacent to the lesions. The ROIs were copied to the qCBV map, and the mean value of ROIs represented the qCBV of lesions. These works were performed via ITK-SNAP (version 3.8.0, www.itksnap.org) by two neuroradiologists together (with over 10 and 15 years of experience, each), who were blind to the diagnostic results.

Group Assignment of the BMs Before GKRS

A previous study confirmed that a qCBV value of 2.0 ml/100 g was a good cut-off value for distinguishing tumor recurrence and radionecrosis of BM after GKRS (18). In addition, the gray matter in the basal ganglia region was ~2.0 ml/100 g (19). Therefore, we chose this value as the cut-off for separating hyperperfusion lesions and hypoperfusion lesions among untreated BMs. Lesions with a mean qCBV value ≤ 2.0 ml/100 g were considered hypoperfusion BMs, while those over 2.0 ml/100 g were considered hyperperfusion BMs.

Diagnosis of Newly or Enlarged Enhanced Lesions

Although histopathological confirmation is the gold standard for differentiating radionecrosis and tumor recurrence of BMs after GKRS, it can be obtained only in a small group of patients. Radiographic and clinical assessments are the most commonly used identification methods (17). Patients' conditions and lesions were thereafter evaluated based on clinical manifestations and routine MR imaging every 3 months. We made the final diagnosis of radiation necrosis when the target lesion showed complete response, partial response, or stable disease depending on the RANO-BM method in subsequent follow-up MR images after a minimum of 6 months (median 12.5 months, range: 6–21 months). If the lesion presented with progression on serial MR examination and the patient's neurological condition deteriorated progressively, we diagnosed the case as tumor recurrence. Clinical assessments were performed by a neurosurgeon (with 12 years of experience), and radiographic assessments were performed by a neuroradiologist (with 18 years of experience). Divergence between clinical and radiographic assessments was resolved by stereotactic biopsy or craniotomy. In addition, the change in qCBV (ΔqCBV) between untreated qCBV ($qCBV_{pre}$) and posttreated qCBV ($qCBV_{post}$) was also calculated, which is defined as $\Delta qCBV = qCBV_{post} - qCBV_{pre}$.

Statistical Analysis

The Kolmogorov–Smirnov test was used to check for the normal distribution of data. Differences in normally distributed data were tested using an unpaired *t* test; non-normally distributed variables were tested using the Mann–Whitney U test. Differences in count variables were tested using the chi-squared test. The difference in qCBV between untreated and recurrent lesions was tested using a paired *t* test. The DeLong test was performed to evaluate the difference in the ROCs. A two-sided *p*-value < 0.05 was considered significantly different.

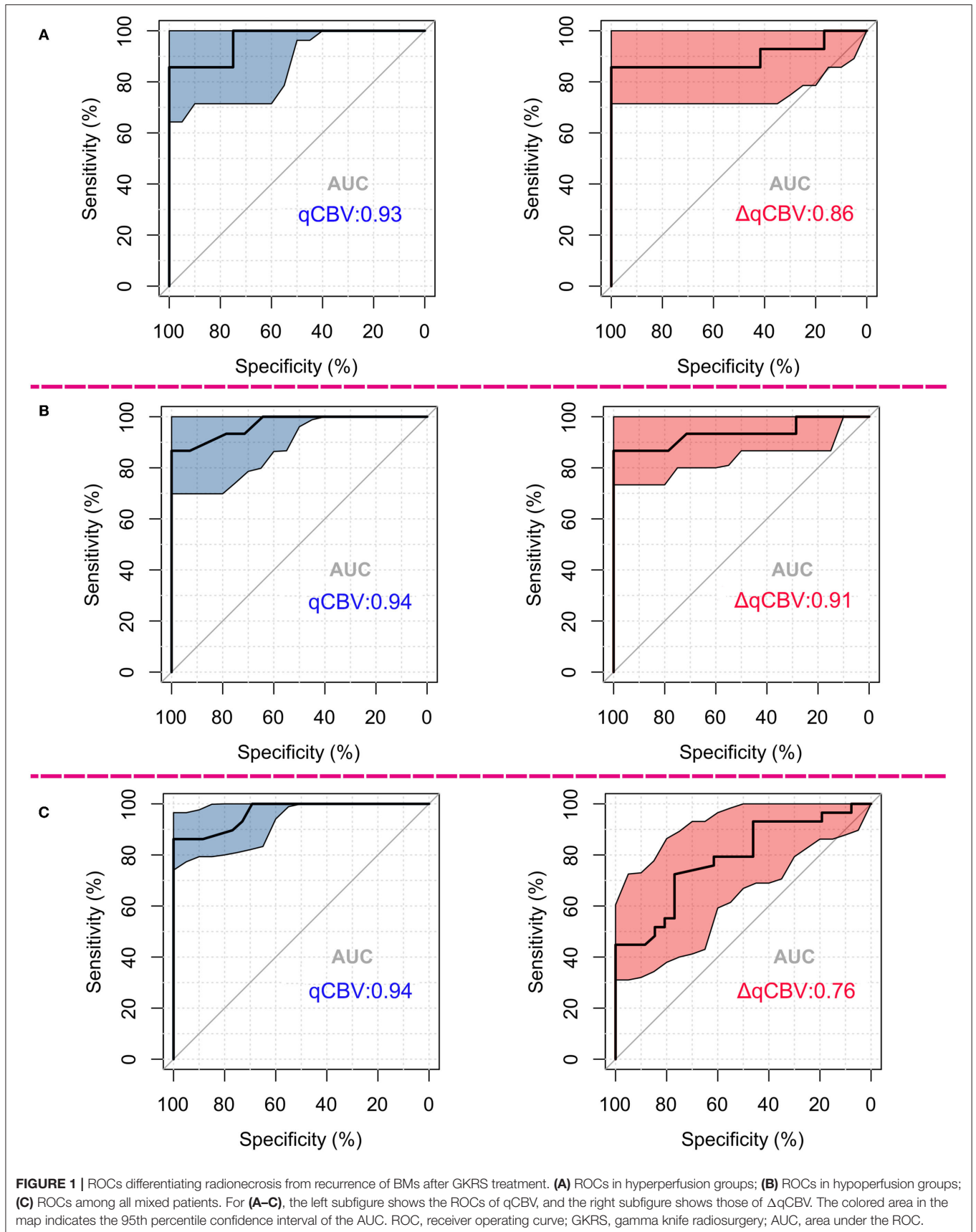


TABLE 4 | The detailed information of ROC analysis.

	AUC	Accuracy	Specificity	Sensitivity	PPV	NPV
qCBV						
Hyperperfusion	0.93	0.89	0.97	0.83	0.97	0.83
Hypoperfusion	0.94	0.90	0.96	0.84	0.97	0.85
All	0.94	0.90	0.97	0.83	0.97	0.84
ΔqCBV						
Hyperperfusion	0.86	0.89	0.97	0.83	0.97	0.83
Hypoperfusion	0.91	0.90	0.97	0.84	0.97	0.84
All	0.76	0.72	0.74	0.69	0.75	0.68

All calculations were performed using SPSS (Statistics version 20, IBM, Armonk, NY).

RESULTS

Study Population

Among the 55 enrolled patients, 29 patients (mean age: 61.3 ± 9.4 years old; male/female: 13/16) were assigned to the group of hypoperfusion BMs, and 26 patients (mean age: 58 ± 10.4 years old; male/female: 14/12) were assigned to the group of hyperperfusion BMs. In addition, 15 and 14 cases were diagnosed as recurrence and radionecrosis in the hypoperfusion BM group, respectively. Fourteen and 12 patients were diagnosed with recurrence and radionecrosis, respectively, in the hypoperfusion BM group. Finally, eight patients (8/29, 27.6%) with recurrence and four patients with radionecrosis (4/26, 15.5%) were diagnosed by stereotactic biopsy or craniotomy. The patients were diagnosed by the depending on the RANO-BM method in subsequent follow-up MR images after a minimum of 6 months. Detailed information on the entire enrolled population is summarized in **Table 1**. The underlying histological subtypes of the primary tumors are summarized in **Table 2**.

Comparisons Between Hyperperfusion and Hypoperfusion Groups

The mean qCBV between untreated and recurrent lesions in the hypoperfusion group was significantly different (1.40 ± 0.32 ml/100 g vs. 3.0 ± 0.58 ml/100 g, $p < 0.001$), and that in the hyperperfusion group was not (3.18 ± 0.68 ml/100 g vs 2.89 ± 0.58 ml/100 g, $p = 0.254$). The mean qCBV between the hyperperfusion and hypoperfusion groups was not significantly different with recurrence ($p = 0.62$) or radionecrosis ($p = 0.45$). In addition, the mean Δ qCBV between the two groups was significantly different with recurrence and radionecrosis (both $p < 0.001$). The detailed results of comparisons between the two groups are summarized in **Table 3**.

Diagnostic Performance in Two Groups and All Patients

The diagnostic performance of qCBV in the two groups and all patients was explored first. qCBV had a similar

diagnostic performance in the two groups and all patients. In addition, Δ qCBV performed worse than qCBV. Furthermore, Δ qCBV in all patients performed worst. The ROC curves of qCBV and Δ qCBV under the three conditions are summarized in **Figure 1**. Detailed information on the ROC analysis is summarized in **Table 4**. Examples of hyperperfusion BMs and hypoperfusion BMs are shown in **Figures 2, 3**.

DISCUSSION

DSC-PWI plays an important role in the differential diagnosis between radionecrosis and tumor recurrence of BMs after GKRS treatment. However, the performance of quantitative DSC-PWI in hyperperfusion and hypoperfusion BMs has not been investigated separately. Our results demonstrated that quantitative DSC-PWI was feasible to separate radionecrosis from recurrence of BMs after GKRS treatment for both kinds of BMs. In addition, both kinds of BMs appear as hyperperfusion when recurring.

Unlike high-grade gliomas, BMs are not always hyperperfused. Traditionally, BMs from lung and breast cancer, which are the most common causes of BMs, have been treated as hypoperfusion lesions (9). Those from kidney cancer and melanoma are treated as hyperperfusion lesions (8). In this study, however, some BMs from lung and breast cancer presented as hyperperfusion lesions, while BMs from melanoma can also present as hypoperfusion lesions. In addition, all of the BMs from kidney cancer presented with hyperperfusion, which is consistent with a previous study (5, 10). The results may reveal heterogeneous perfusion conditions in BMs. We observed that most of [23 of 26] these hyperperfusion lesions were solid or solid-cystic, while most [24 of 29] hypoperfusion lesions were cystic or unsolid. These results may indicate that the solid part of BMs could result in high overexpression of VEGF (13). Therefore, according to our findings, evaluation of the perfusion conditions of untreated BMs referring only to the origination of the tumor is not correct. MR perfusion should be performed when evaluating the perfusion conditions of untreated BMs.

The feasibility of DSC-PWI in distinguishing radionecrosis from recurrence of BMs after radiotherapy has been validated by many previous studies (5, 9–11). Few studies have reported the performance of quantitative DSC-PWI [18]. In addition, no studies have explored the performance of quantitative DSC-PWI in hyperperfusion and hypoperfusion BMs separately. Our results showed that quantitative DSC-PWI had good separation performance in both hyperperfusion and hypoperfusion BMs, as well as in a mixed population. Interestingly, for the preliminary hypoperfusion BMs, most of them showed a greatly improved qCBV value when they recurred. This means that the hypoperfusion BMs would transform to hyperperfusion BMs when they recur. The reasons for the change in perfusion conditions in hypoperfusion BMs may be that radiotherapy induced VEGF overexpression in tumor

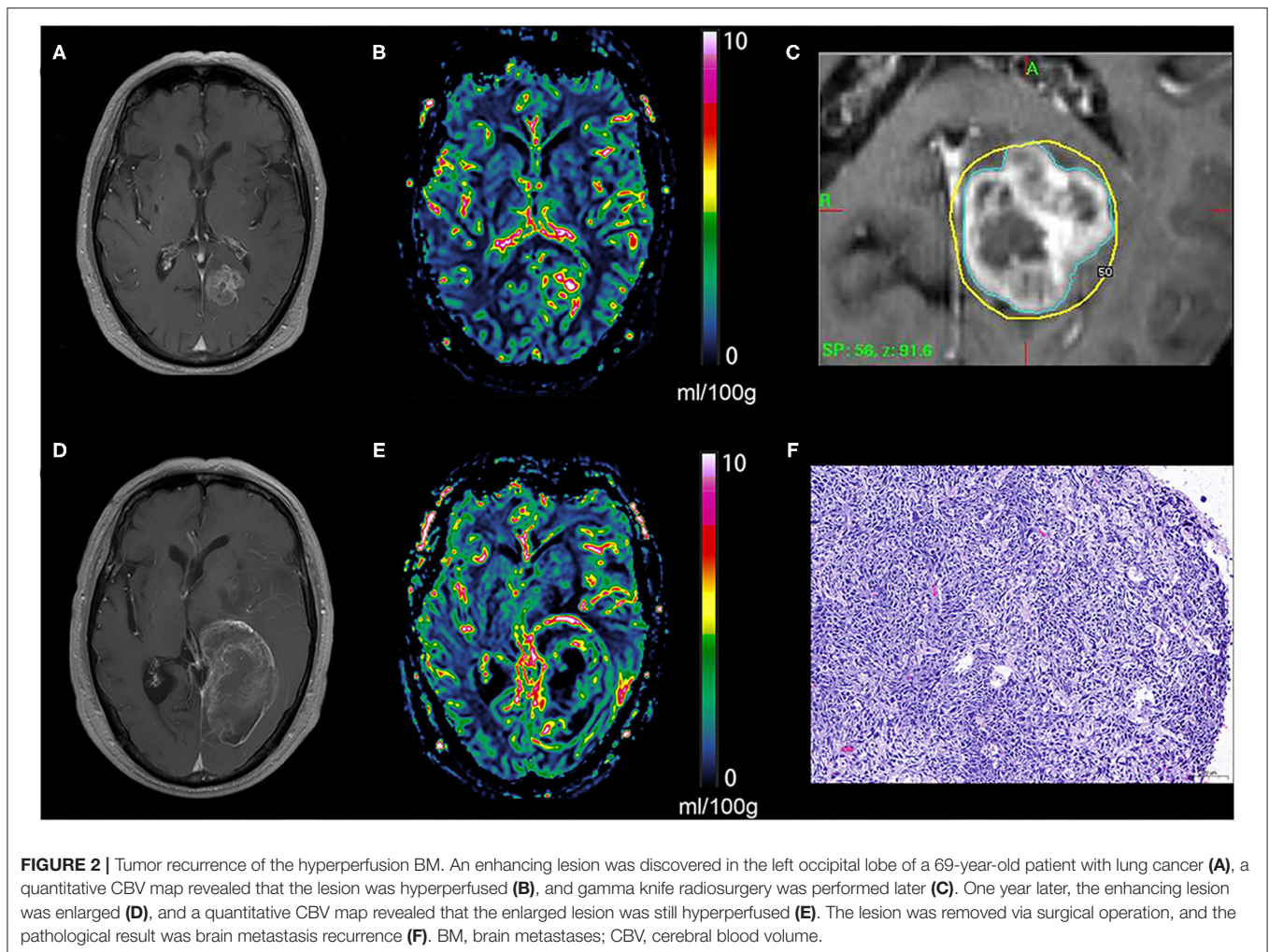


FIGURE 2 | Tumor recurrence of the hyperperfusion BM. An enhancing lesion was discovered in the left occipital lobe of a 69-year-old patient with lung cancer (A), a quantitative CBV map revealed that the lesion was hyperperfused (B), and gamma knife radiosurgery was performed later (C). One year later, the enhancing lesion was enlarged (D), and a quantitative CBV map revealed that the enlarged lesion was still hyperperfused (E). The lesion was removed via surgical operation, and the pathological result was brain metastasis recurrence (F). BM, brain metastases; CBV, cerebral blood volume.

cells or that radiotherapy-resistant tumor cells transformed to higher malignancy with VEGF overexpression when they recurred.

Due to the limitation of artery input functions (AIFs) of DSC-PWI, it could be a challenge to use this technology as a quantitative approach to evaluate the perfusion conditions of brain tumors. Bookend DSC-PWI provided an AIF-independent approach to solve this problem (15). With the help of the Bookend technique, quantitative CBV is feasible in the longitudinal and transversal assessment of perfusion conditions of BMs. Our results demonstrated that the difference (Δ qCBV) between untreated qCBV and posttreated qCBV at diagnosis did not perform better than qCBV in separating radionecrosis from tumor recurrence. Moreover, Δ qCBV is not applicable in a mixed population because it had the worst performance under this condition. The reason may be that the preliminary hyperperfusion BMs would still be hyperperfusion BMs when diagnosed as recurrence, and the preliminary hypoperfusion BMs would still be hypoperfusion BMs when diagnosed as radionecrosis,

and a large overlap would be inevitable under both kinds of conditions.

Some limitations should be addressed here. First, the size of the study population was relatively small, and further studies with larger populations should be performed to validate our findings. Second, only a limited number of patients were validated by pathological results because only a small portion of BMs need neurosurgical intervention after GKRS. In addition, for patients with a probability of radionecrosis, this is an inherent dilemma in clinical treatment because the risk of possible complications of biopsy might outweigh the benefits of histopathological diagnosis (1).

In conclusion, hypoperfusion BMs transform to hyperperfusion BMs when they recur. Quantitative CBV could still be feasible to distinguish radionecrosis from tumor recurrence in both hyperperfusion and hypoperfusion BMs after GKRS treatment. Further studies with larger and multicentre cohort validation should be performed to validate our findings.

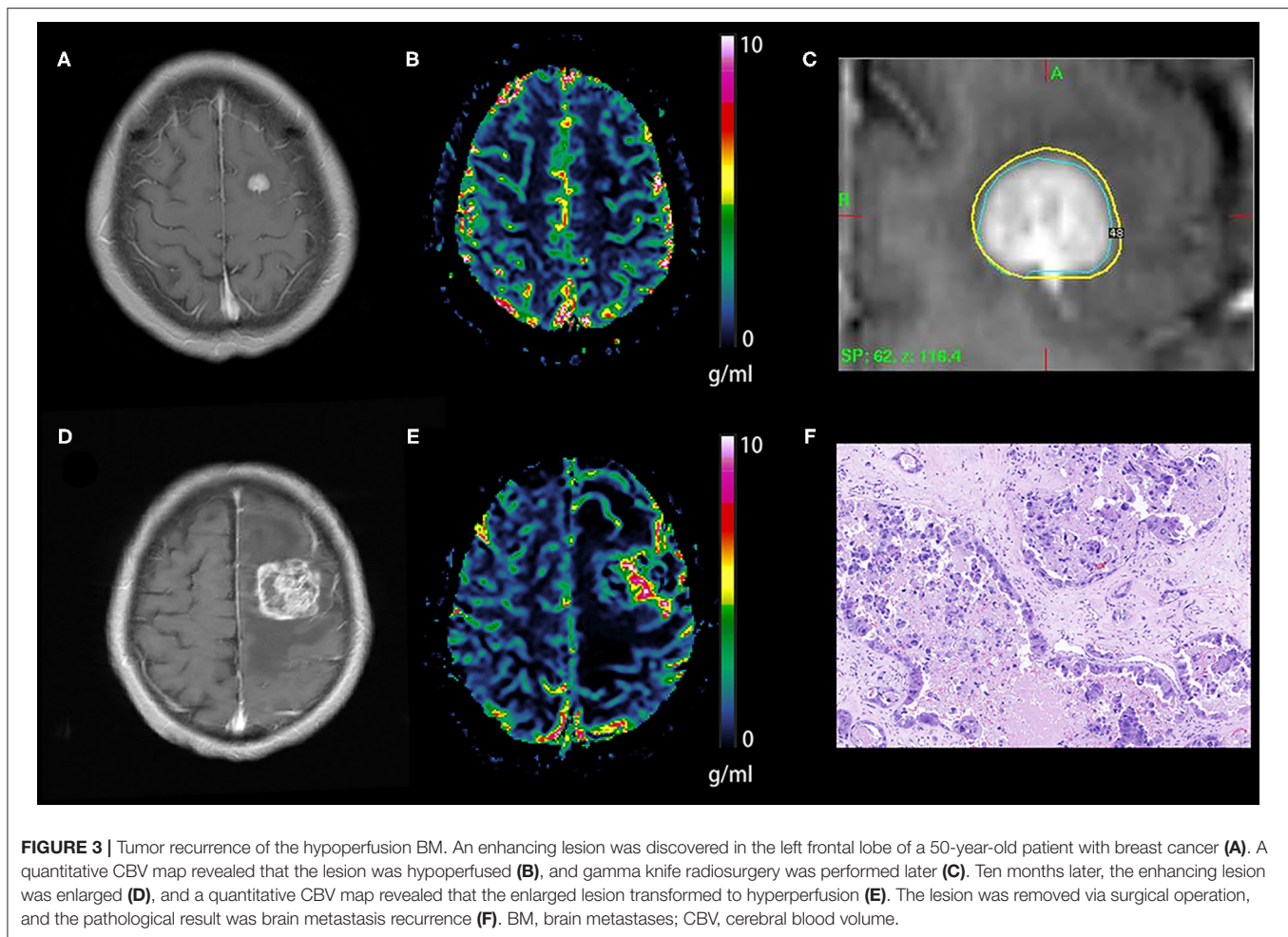


FIGURE 3 | Tumor recurrence of the hypoperfusion BM. An enhancing lesion was discovered in the left frontal lobe of a 50-year-old patient with breast cancer (A). A quantitative CBV map revealed that the lesion was hypoperfused (B), and gamma knife radiosurgery was performed later (C). Ten months later, the enhancing lesion was enlarged (D), and a quantitative CBV map revealed that the enlarged lesion transformed to hyperperfusion (E). The lesion was removed via surgical operation, and the pathological result was brain metastasis recurrence (F). BM, brain metastases; CBV, cerebral blood volume.

DATA AVAILABILITY STATEMENT

The raw data supporting the conclusions of this article will be made available by the authors, without undue reservation.

ETHICS STATEMENT

The studies involving human participants were reviewed and approved by Shandong Provincial Hospital Affiliated to Shandong First Medical University. The patients/participants provided

their written informed consent to participate in this study.

AUTHOR CONTRIBUTIONS

MY and ZY: guarantor of integrity of the entire study. YY and NA: study concepts, design, and manuscript preparation. WQ and LY: literature research and clinical studies. YY and MY: experimental studies/data analysis. NA and ZY: statistical analysis. YY, NA, ZZ, LY, WQ, MY, and ZY: manuscript editing. All authors contributed to the article and approved the submitted version.

REFERENCES

- Patel TR, Knisely JP, Chiang VL. Management of brain metastases: surgery, radiation, or both? *Hematol Oncol Clin North Am.* (2012) 26:933–47. doi: 10.1016/j.hoc.2012.04.008
- Brown PD, Ballman KV, Cerhan JH, Anderson SK, Carrero XW, Whitton AC, et al. Postoperative stereotactic radiosurgery compared with whole brain radiotherapy for resected metastatic brain disease (NCCTG N107C/CEC.3): A multicentre, randomised, controlled, phase 3 trial. *Lancet Oncol.* (2017) 18:1049–60. doi: 10.1016/S1470-2045(17)30441-2
- Stockham AL, Tievsky AL, Koyfman SA, Reddy CA, Suh JH, Vogelbaum MA, et al. Conventional MRI does not reliably distinguish radiation necrosis from tumor recurrence after stereotactic radiosurgery. *J Neurooncol.* (2012) 109:149–58. doi: 10.1007/S11060-012-0881-9
- Dhermain FG, Hau P, Lanfermann H, Jacobs AH, van den Bent MJ. Advanced MRI and PET imaging for assessment of

- treatment response in patients with gliomas. *Lancet Neurol.* (2010) 9:906–20. doi: 10.1016/S1474-4422(10)70181-2
5. Mitsuya K, Nakasu Y, Horiguchi S, Harada H, Nishimura T, Bando E, et al. Perfusion weighted magnetic resonance imaging to distinguish the recurrence of metastatic brain tumors from radiation necrosis after stereotactic radiosurgery. *J Neurooncol.* (2010) 99:81–8. doi: 10.1007/S11060-009-0106-Z
 6. Verma N, Cowperthwaite MC, Burnett MG, Markey MK. Differentiating tumor recurrence from treatment necrosis: a review of neuro-oncologic imaging strategies. *Neuro Oncol.* (2013) 15:515–34. doi: 10.1093/Neuonc/Nos307
 7. Shah R, Vattoth S, Jacob R, Manzil FF, O'Malley JP, Borghei P, et al. Radiation necrosis in the brain: imaging features and differentiation from tumor recurrence. *Radiographics.* (2012) 32:1343–59. doi: 10.1148/rg.325125002
 8. Barajas RJ, Cha S. Metastasis in adult brain tumors. *Neuroimaging Clin N Am.* (2016) 26:601–20. doi: 10.1016/j.nic.2016.06.008
 9. Essig M, Waschkes M, Wenz F, Debus J, Hentrich HR, Knopp MV, et al. Assessment of brain metastases with dynamic susceptibility-weighted contrast-enhanced MR imaging: initial results. *Radiology.* (2003) 228:193–9. doi: 10.1148/Radiol.2281020298
 10. Weber MA, Thilmann C, Lichy MP, Gunther M, Delorme S, Zuna I, et al. Assessment of irradiated brain metastases by means of arterial spin-labeling and dynamic susceptibility-weighted contrast-enhanced perfusion MRI: initial results. *Invest Radiol.* (2004) 39:277–87. doi: 10.1097/01.rli.0000119195.50515.04
 11. Hoefnagels FW, Lagerwaard FJ, Sanchez E, Haasbeek CJ, Knol DL, Slotman BJ, et al. Radiological progression of cerebral metastases after radiosurgery: assessment of perfusion MRI for differentiating between necrosis and recurrence. *J Neurol.* (2009) 256:878–87. doi: 10.1007/S00415-009-5034-5
 12. Leeman JE, Clump DA, Flickinger JC, Mintz AH, Burton SA, Heron DE. Extent of perilesional edema differentiates radionecrosis from tumor recurrence following stereotactic radiosurgery for brain metastases. *Neuro Oncol.* (2013) 15:1732–8. doi: 10.1093/Neuonc/Not130
 13. Barbier EL. T2*-weighted perfusion MRI. *Diagn Interv Imaging.* (2013) 94:1205–9. doi: 10.1016/j.Diii.2013.06.007
 14. Shin W, Horowitz S, Ragin A, Chen Y, Walker M, Carroll TJ. Quantitative cerebral perfusion using dynamic susceptibility contrast MRI: evaluation of reproducibility and age- and gender-dependence with fully automatic image postprocessing algorithm. *Magn Reson Med.* (2007) 58:1232–41. doi: 10.1002/mrm.21420
 15. Carroll TJ, Horowitz S, Shin W, Mouannes J, Sawlani R, Ali S, et al. Quantification of cerebral perfusion using the “bookend technique”: an evaluation in CNS tumors. *Magn Reson Imaging.* (2008) 26:1352–9. doi: 10.1016/j.mri.2008.04.010
 16. Srour JM, Shin W, Shah S, Sen A, Carroll TJ. SCALE-PWI: a pulse sequence for absolute quantitative cerebral perfusion imaging. *J Cereb Blood Flow Metab.* (2011) 31:1272–82. doi: 10.1038/jcbfm.2010.215
 17. Lin NU, Lee EQ, Aoyama H, Barani IJ, Barboriak DP, Baumert BG, et al. Response assessment criteria for brain metastases: proposal from the RANO group. *Lancet Oncol.* (2015) 16:E270–8. doi: 10.1016/S1470-2045(15)70057-4
 18. Wang B, Zhao B, Zhang Y, Ge M, Zhao P, Sun N, et al. Absolute CBV for the differentiation of recurrence and radionecrosis of brain metastases after gamma knife radiotherapy: a comparison with relative CBV. *Clin Radiol.* (2018) 73:751–8. doi: 10.1016/j.Crad.2018.04.006
 19. Allmendinger AM, Tang ER, Lui YW, Spektor V. Imaging of stroke: part 1, perfusion CT—overview of imaging technique, interpretation pearls, and common pitfalls. *AJR Am J Roentgenol.* (2012) 198:52–62. doi: 10.2214/AJR.10.7255

Conflict of Interest: The authors declare that the research was conducted in the absence of any commercial or financial relationships that could be construed as a potential conflict of interest.

Publisher's Note: All claims expressed in this article are solely those of the authors and do not necessarily represent those of their affiliated organizations, or those of the publisher, the editors and the reviewers. Any product that may be evaluated in this article, or claim that may be made by its manufacturer, is not guaranteed or endorsed by the publisher.

Copyright © 2022 Yunqi, Aihua, Zhiming, Yingchao, Qiang, Yang and Yi. This is an open-access article distributed under the terms of the Creative Commons Attribution License (CC BY). The use, distribution or reproduction in other forums is permitted, provided the original author(s) and the copyright owner(s) are credited and that the original publication in this journal is cited, in accordance with accepted academic practice. No use, distribution or reproduction is permitted which does not comply with these terms.